

Structure-Based Ligandability Exploration of a G-Quadruplex-Forming Sequence from the *Pseudomonas aeruginosa* Genome

Martina Fiabane,[▽] Chiara Platella,[▽] Fabiana Diaco,[▽] Cristiano Biancucci, Andrea Calcaterra, Domenica Musumeci, Guido Antonelli, Ombretta Turriziani, Bruno Botta, Daniela Montesarchio,* and Mattia Mori*



Cite This: <https://doi.org/10.1021/acsmedchemlett.5c00428>



Read Online

ACCESS |



Metrics & More



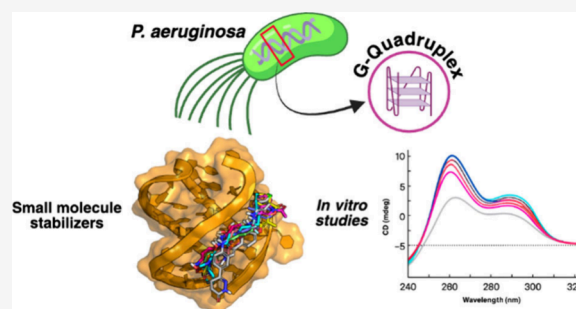
Article Recommendations



Supporting Information

ABSTRACT: Bacterial G-quadruplexes (G4s) are related to survival and resistance mechanisms in several pathogens, making them attractive targets for innovative antimicrobials. However, little structural and ligand binding information is available so far. Based on the structure of the TET22 G4 from *Pseudomonas aeruginosa*, a structure-based multidisciplinary approach was applied here to assess its ligandability. A docking-based virtual screening allowed the identification of the putative TET22 groove binders 1–13 that were evaluated in biophysical and biological assays. Circular dichroism (CD) confirmed that compounds 1–13 and the reference ligand pyridostatin (PDS) bind and stabilize TET22, each displaying a differential preference for parallel or antiparallel/hybrid topology. Notably, compounds 5 and 7, the most effective ligands for TET22 G4, proved to be unable to stabilize a human telomeric G4 model used as a selectivity control. Microbiology evaluation returned weak efficacy for compounds 1–13, whereas a minimum inhibitory concentration (MIC) of 100 μ M was obtained for the reference compound PDS, indicating that TET22 stabilization stronger than that provided by compounds 1–13 is required to observe a detectable antimicrobial efficacy. Surprisingly, some well-known human G4 binders were fully inactive.

KEYWORDS: G-quadruplex, *Pseudomonas aeruginosa*, stabilizers, antibacterial agents, TET22



The World Health Organization (WHO) has highlighted antimicrobial resistance (AMR) as a global health threat responsible for around 700,000 deaths per year worldwide, with severe outcomes in the next two decades.¹ Indeed, recent statistics underscore the remarkable increase in AMR spread and related issues, including mortality rates, which are expected to rise to several million deaths by 2050, thus surpassing cancer-related deaths.^{2–4} Among the limits that are currently facilitating AMR spread in clinical and civil settings, the lack of novel and innovative antibacterial drugs is surely one of the most critical issues. Starting in the 1990s, a serious decline in antibiotic research and development (R&D) was recorded, mostly due to several factors including (i) the lack of funding by governments and health institutions, (ii) the low success rate of novel antibiotics in the clinical pipeline, and (iii) the low economic revenue from the commercialization of a new antibiotics compared to R&D investments.⁵ These criticisms have contributed to the progressive abandonment of the antibacterial discovery field by several pharmaceutical companies in favor of more remunerative therapeutic areas, such as oncology and diabetes. As a result, in the last decades, only a few antibiotics have been developed with most of them corresponding only to slight chemical modifications of

available antibiotic drugs, to which most bacteria have already developed resistance mechanisms.^{6–9}

Recently, some efforts have been spent in the design and development of adjuvants, i.e., chemical entities able to revert or interfere with the AMR mechanisms and to resensitize pathogens toward drugs for which they have developed drug resistance. Despite some success, for example, the development of β -lactamase or carbapenemase inhibitors (e.g., the taniborbactam–cefepime combination, currently pending approval by FDA),¹⁰ very few examples of novel leads that can directly impair bacterial growth and/or replication through novel mechanisms of action, endowed with a low susceptibility to drug resistance, are available.¹¹

In this context, our research interests are aimed at the identification and validation of novel putative targets for the development of antibiotics with a high bar to resistance.

Received: July 12, 2025

Revised: July 28, 2025

Accepted: August 1, 2025

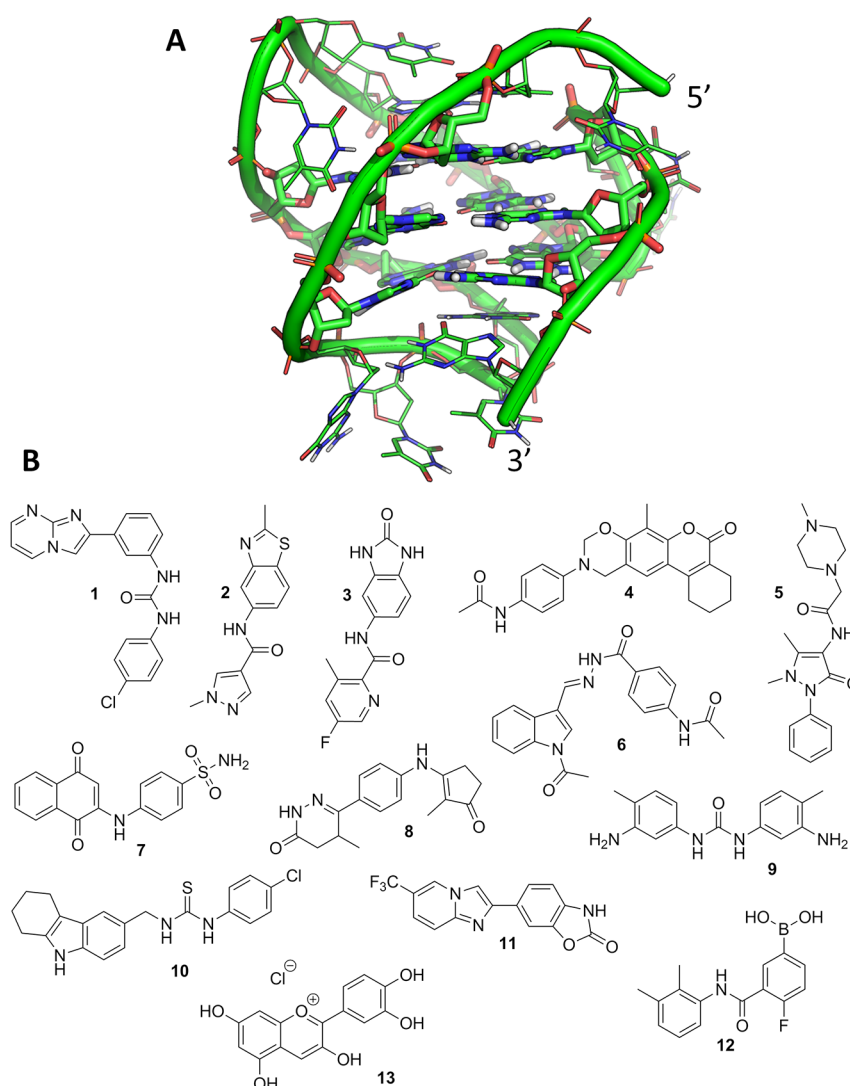


Figure 1. (A) NMR structure of TET22 (PDB-ID: 186D; the first NMR model is shown); (B) chemical structure of small molecules 1–13 here selected as putative TET22 G4 binders from virtual screening.

Specifically, noncanonical nucleic acid motifs are highly attractive because they (i) are readily available by bioinformatic analyses of bacterial genome sequences, (ii) have lower tendency to mutate compared to proteins, and (iii) play a crucial role in several bacterial functions including growth, replication, and drug-resistance.¹² Among them, we focused on G-quadruplexes (G4s), which are secondary structures of both DNA and RNA formed in genome sequences rich in guanine nucleotides.^{13–16} Extensive knowledge is available for human G4s, which are profitable targets for anticancer drug discovery, as highlighted by the running Phase I clinical trial on the G4 stabilizer QN-302 (ClinicalTrials.gov ID NCT06086522).^{17,18} In contrast, the interest toward bacterial G4s arose much later, and very little information is available on the structure and functions of these putative targets for the development of antibacterial agents. Particularly, the lack of three-dimensional structures along with the high polymorphism of G4s currently hampers the application of well-established structure-based methods for the identification of hit and lead stabilizers of bacterial G4s. Moreover, both Gram-positive and -negative bacteria have a thick cell wall that strongly restricts small molecule entry by passive permeation, which represents a

further challenge in the design of small molecule modulators of bacterial G4s compared to human G4s. Nonetheless, the possibility to rapidly identify putative G4-forming sequences in bacterial genomes by bioinformatic tools, coupled with the relatively high-throughput access to genome sequences by next-generation sequencing (NGS) methods, makes G4s promising drug targets, especially for preparedness against possible future epidemics/pandemics.

In this frame, we aimed at exploring the druggability of bacterial G4s by small molecules through the combination of computational modeling tools, biophysical assays, and microbiological investigations. Due to the limited availability of bacterial G4 structural details, we focused on the G4-forming sequence TET22 from the pathogen *Pseudomonas aeruginosa*, although formerly extrapolated from the *Tetrahymena* genome, whose structure was solved by nuclear magnetic resonance (NMR).¹⁹ Notably, *P. aeruginosa* is an opportunistic Gram-negative pathogen responsible for hospital-acquired infections, particularly ventilator-associated pneumonia and cystic fibrosis.^{20,21} Treatment of *P. aeruginosa* infections has become increasingly challenging due to its ability to develop resistance toward many antibiotics, including aminoglycosides, quino-

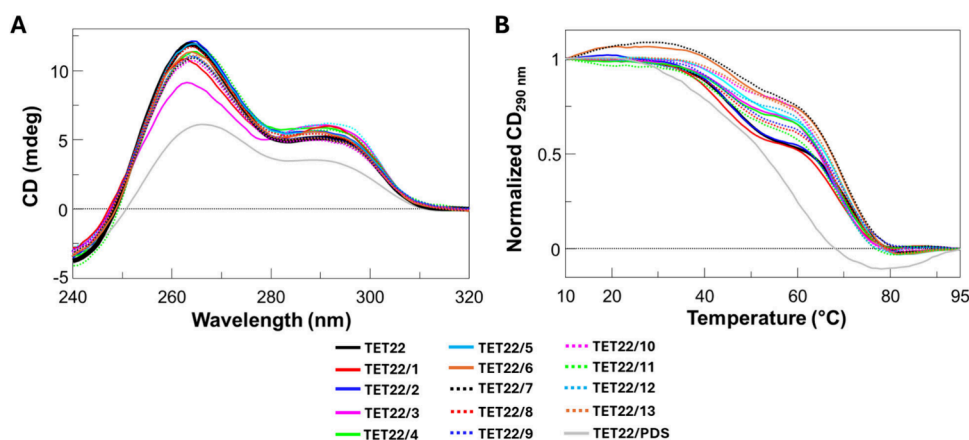


Figure 2. (A) CD spectra of 2 μM solutions of TET22 in 0.5 mM KCl, 0.5 mM potassium phosphate (pH 7) in the absence or presence of compounds 1–13 and PDS (10 equiv). (B) Normalized CD melting curves of 2 μM solutions of TET22 in 0.5 mM KCl, 0.5 mM potassium phosphate (pH 7) in the absence or presence of compounds 1–13 and PDS (10 equiv), recorded at 290 nm.

loners, and β -lactams through several different mechanisms such as efflux pump expression, production of drug-degrading enzymes, or acquisition of resistance genes through horizontal gene transfer.^{22–25} For these reasons, *P. aeruginosa* is included in the high-priority list of pathogens released by the WHO in 2017 and recently updated in 2024,^{1,26} for which the development of new antibiotics or alternative therapeutic strategies is urgently needed.

The NMR solved structure of TET22 G4, whose sequence is 5'-(TTGGGG)₄-3', also described as (T₂G₄)₄, is composed of three G-tetrads (Figure 1A), two of which have an *anti-anti-anti-syn* configuration of the guanines, whereas the third G-tetrad has a *syn-syn-syn-anti* configuration, with the G-tetrads being connected by a GT₂G loop, a central T₂G loop, and a T₂ loop, resulting in a G4 hybrid topology.¹⁹ Structural features of this G4 offer peculiar strand directions and groove widths, allowing the possibility of exploring multiple binding sites in the search for small molecule TET22 stabilizers.

Here, the ligandability of *P. aeruginosa* TET22 G4 was first explored by a structure-based virtual screening. To this aim, the MolPort collection containing more than 10 million compounds was downloaded and customized through application of a number of chemoinformatic filters. Specifically, we removed compounds available by custom synthesis or not in stock, and we retained only compounds available in stock for a total of 4,818,666 molecules. Then, additional filters were applied to retain small molecules having the following features: (i) molecular weight in the range 200–500 Da to align with lead-likeness; (ii) formal charge in the range 0–2 to promote electrostatic attractive interactions with negatively charged nucleic acids; (iii) absence of carboxylic acid moieties to avoid electrostatic repulsions with the phosphate backbone of nucleic acids; (iv) up to 1 chiral center to avoid experimental tests on complex mixtures of isomers. After this preliminary step, the final sublibrary was composed of 3,540,420 molecules, which were prepared for virtual screening by conversion into a 3D format, assignment of the ionization state for pH = 7.4, and energy minimization according to a standardized procedure.^{27–29} The sublibrary was docked against the whole accessible surface of TET22 by the software GOLD, using the Chemscore function for docking and scoring purposes.³⁰ Docking complexes were further relaxed by energy minimization. Docking results were analyzed by a combination of score, visual inspection of the docking pose, and chemical diversity,

which led to the selection of compounds 1–13 (Figure 1B) located in the TET22 G4 groove for biophysical and microbiology investigations. It is worth noting that small molecules stacking on top of terminal G-tetrads are highly effective although poorly specific, being able to typically bind all kinds of G4 structures as well as the most abundant duplex DNA.³¹ In contrast, groove binders are thought to be more selective toward a specific G4 topology, thus allowing potential discrimination between bacterial and human G4s. Finally, G4 groove binders are generally endowed with a higher drug-likeness compared to end-stackers, as confirmed by the most important physicochemical and toxicology descriptors predicted by SwissADME (Supporting Information, Tables S1 and S2).^{12,13,32–36}

Circular dichroism (CD) studies were performed to evaluate the effects of the selected compounds 1–13 on the topology and thermal stability of the target TET22 G4. Ligand effects on the G4 conformation and overall structuring degree were evaluated by incubating TET22 with each compound and recording CD spectra (Figure 2A). In parallel, the thermal stability of free and ligand-bound TET22 was evaluated by monitoring the CD signal at 290 and 260 nm, characteristic maxima for the different G4 topologies of this sequence (see below), on increasing the temperature (Figure 2B and Table 1). Furthermore, three-dimensional melting curves for the free TET22 G-quadruplex and TET22/ligand systems were also obtained by recording whole CD spectra as a function of temperature (Figures S1–S4).

In order to optimize the experimental conditions for this study, the thermal stability of free TET22 was first tested in several conditions mimicking the K⁺ concentration and pH of the bacterial environment (Supporting Information, Figure S1). The following buffered solutions were used: (i) 20 mM KCl, 5 mM potassium phosphate (pH 7), (ii) 2 mM KCl, 0.5 mM potassium phosphate (pH 7), and (iii) 0.5 mM KCl, 0.5 mM potassium phosphate (pH 7). Considering that buffer (i) provides TET22 with a thermal stability that prevents the accurate determination of its melting temperature ($T_m > 80$ °C), in agreement with literature data,³⁷ buffers (ii) and (iii) were selected, providing more suitable conditions for ligand binding studies. Moreover, considering that CD spectra recorded in the presence of buffers (ii) and (iii) were almost identical (Supporting Information, Figure S1A, red and blue curves), buffer (iii) was selected for melting experiments due

Table 1. Melting Temperature (T_m) Values of TET22 in 0.5 mM KCl, 0.5 mM Potassium Phosphate (pH 7) in the Absence or Presence of Compounds 1–13 and PDS (10 equiv) as Measured by CD Melting Experiments Recorded at 290 or 260 nm^a

compound	TET22 (290 nm) – hybrid or antiparallel		TET22 (290 nm) – hybrid or antiparallel		TET22 (260 nm) – parallel	
	$T_m \pm 1$ (°C)	ΔT_m (°C)	$T_m \pm 1$ (°C)	ΔT_m (°C)	$T_m \pm 1$ (°C)	ΔT_m (°C)
no ligand	45		69		48	
1	44	–1	68	–1	49	+1
2	45	0	69	0	49	+1
3	46	+1	68	–1	48	0
4	45	0	68	–1	49	+1
5	48	+3	70	+1	49	+1
6	47	+2	70	+1	48	0
7	49	+4	69	0	49	+1
8	46	+1	69	0	49	+1
9	45	0	69	0	49	+1
10	46	+1	68	–1	48	0
11	45	0	68	–1	48	0
12	46	+1	68	–1	48	0
13	47	+2	69	0	48	0
PDS	58	+13	<i>b</i>	<i>b</i>	69	+21

^a $\Delta T_m = T_m(\text{DNA/ligand, 1:10}) - T_m(\text{free DNA})$. ^bNot determined.

to the higher resolution of the two inflection points in the melting curve (Supporting Information, Figure S1B, red and blue curves).

Deconvolution analysis of both CD spectra and CD melting curves of TET22 proved that, under the conditions explored herein, this G4 sequence folds into three different topologies, i.e., parallel, hybrid, and antiparallel (sorted by their relative abundance), which are in equilibrium in solution (Tables 1 and 2), in agreement with a previous work.³⁸ Thus, melting

Table 2. Singular Value Decomposition (SVD) Analysis of CD Spectra of 2 μM Solutions of TET22 in 0.5 mM KCl, 0.5 mM Potassium Phosphate (pH 7) in the Absence or Presence of Compounds 1–13 and PDS (10 equiv), Performed by the Software Developed by del Villar-Guerra et al.^{40a}

compound	antiparallel	hybrid	parallel
no ligand	7.5	43.2	50.3
1	7.3	59.9	33.9
2	1.8	52.7	46.4
3	14.7	49.3	37.0
4	3.8	55.6	41.6
5	6.0	54.2	40.8
6	5.6	57.7	37.6
7	5.9	55.1	40.0
8	5.4	50.6	45.0
9	13.7	43.5	43.8
10	9.2	49.9	39.9
11	10.8	44.6	44.1
12	4.4	57.0	39.6
13	13.3	53.0	34.7
PDS	29.8	32.3	36.8

^aThe predicted relative abundance of G4 topologies is reported in % values.

temperatures were estimated for each TET22 topology (parallel, $T_m = 48$ °C; hybrid or antiparallel (inflection point 1), $T_m = 45$ °C; hybrid or antiparallel (inflection point 2), $T_m = 69$ °C).

Optimized experimental conditions were then used for CD titration and melting experiments on the TET22/ligand systems. Upon incubation of TET22 with 10 equiv of each compound of the investigated set 1–13, relevant changes in the CD spectrum of TET22 were observed in most cases (Figure 2A). In detail, all compounds were able to increase the content of the hybrid topology as well as to decrease the content of the parallel topology compared to free TET22. In contrast, changes in the antiparallel topology were observed only in some cases (Table 2). Significant TET22 stabilizing effects were detected for 5, 6, 7, and 13 on the hybrid or antiparallel G4 topology (Figure 2B and Table 1). The well-known G4 binder pyridostatin (PDS) was used as a positive control. Its binding to TET22 produced a mixture of all three G4 topologies, i.e., parallel, hybrid, and antiparallel, in a similar amount (Table 2), resulting in higher TET22 stabilization compared to 1–13 (Figure 2 and Table 1). Interestingly, PDS was also able to induce a full shift of the TET22 G4 topology mixture to a major parallel G4 fold upon increasing the temperature (Figure S4D), as recently observed by Martin et al. in testing the bisquinolinium PyDH2 analogue of PDS against the G4-forming sequence 5'-G(TTGGGG)₄-3' (TET25) from *Tetrahymena thermophila*.³⁹

Additionally, for the most stabilizing ligands, i.e., 5, 7, and PDS, CD titration and CD melting experiments were performed also with a human telomeric G4 structure model (tel26, 5'-(TTAGGG)₄TT-3') to evaluate the selectivity of these compounds for bacterial vs human G4s (Supporting Information, Figure S5). Notably, while PDS was able to significantly affect both tel26 conformation and stability, 5 and 7 did not perturb the tel26 structure nor affect its thermal stability (Supporting Information, Figure S5 and Table S3), thus evidencing the ability of these ligands to discriminate between bacterial and human G4s. Our findings reinforce the hypothesis that G4 groove binders can result in higher selectivity for a specific bacterial G4 than that of other G4 structures, such as those found in the human genome.

The docking-based binding mode of 5 and 7, which showed selective stabilizing effects on both hybrid/antiparallel and parallel TET22 topologies compared to the hybrid human tel26 G4, was analyzed in more detail. Both compounds can fit the TET22 groove formed between the 5' and 3' ends, and established H-bond interactions with the phosphate backbone and with guanine residues, including those forming the G-tetrads (Figure 3).

Specifically, the 4-aminoantipyrine moiety of 5 was located within the 3' end of TET22 groove, where it was H-bonded to G3 and G23. The *N*-methylpiperazine group of 5 was projected toward the 5' end, establishing a charge-assisted H-bond interaction with T2 (Figure 3A). Compound 7 occupied the same groove as 5, with the quinone moiety being H-bonded to G22, whereas all other H-bonds were established by the sulfamide group to G24 within the 3' end (Figure 3B).

Finally, the antimicrobial potential of compounds 1–13 and PDS was tested against *P. aeruginosa* ATCC 27853. Results showed that most compounds exhibited a smaller decrease in absorbance compared to the positive control PDS at 100 μM (Figure 4). However, no minimum inhibitory concentration

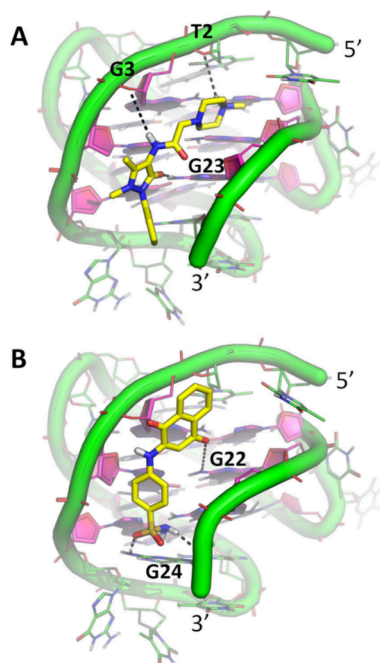


Figure 3. Docking-based binding mode of (A) 5 and (B) 7 within the accessible surface of TET22 G4. TET22 is shown as a green cartoon and lines; guanine nucleotides from G-tetrads are colored in magenta and are shown as filled-ring sticks. Small molecules are shown as yellow sticks; polar interactions are highlighted by black dashed lines. Residues contacted by the small molecules as well as 5' and 3' termini are labeled. The orientation of TET22 shown in Figure 1 is preserved.

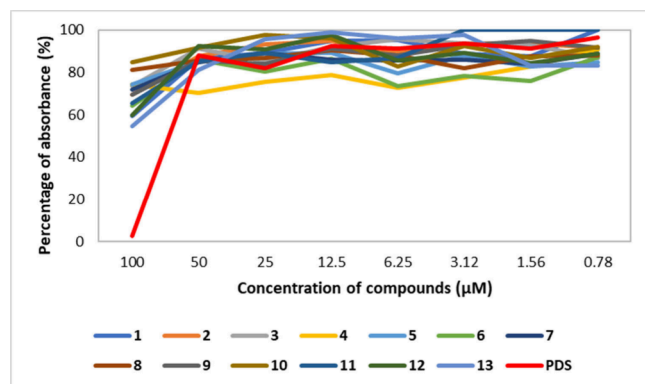


Figure 4. Percentage of absorbance of samples treated with compounds 1–13 and PDS with respect to the positive control for *P. aeruginosa*.

(MIC) could be determined for all compounds, whereas a MIC value of 100 μM was determined for PDS against *P. aeruginosa*. This result is consistent with the stronger effects found for PDS compared to 1–13 determined by CD, thus suggesting that similar stabilizing activity on TET22 as exhibited by PDS is required in order to observe a relevant antimicrobial activity.

To further explore the role of G4 binders against *P. aeruginosa*, the activity of additional and well-known G4 stabilizers BRACO-19, TMPyP4, and RHPS4 was subsequently tested by CD and microbiological assays. CD studies proved that also these ligands, as in the case of PDS, induced a reduction of the CD signal of TET22 (Supporting Information, Figure S6A). However, differently from what was observed for human G4s,⁴¹ we found that BRACO-19,

TMPyP4, and RHPS4 also failed to provide thermal stabilization of TET22 (Supporting Information, Figure S6 and Table S4). Interestingly, BRACO-19, TMPyP4, and RHPS4 proved unable to exert any antimicrobial activity against *P. aeruginosa* (Supporting Information, Figure S7), suggesting that only ligands with a strong effect on TET22 G4 thermal stability, such as PDS, can result in effective antimicrobial agents.

In conclusion, although no antimicrobial activity was detected for 1–13, the efficacy observed for PDS against *P. aeruginosa* corroborates the hypothesis that targeting bacterial G4s such as TET22 might be a promising strategy to develop innovative antimicrobial agents up to drug candidates. In this framework, structure-based approaches might notably enhance the discovery of G4-stabilizing agents and contribute to their optimization up to profitable leads. In targeting the TET22 G4 from *P. aeruginosa*, 1–13 represent valuable starting compounds for the development of more effective, selective, and drug-like G4 stabilizers binding TET22 and, generally, other bacterial G4s.

■ ASSOCIATED CONTENT

Supporting Information

The Supporting Information is available free of charge at <https://pubs.acs.org/doi/10.1021/acsmchemlett.5c00428>.

Additional CD results and spectra of the free and ligand-bound bacterial TET22 G4 and human tel26 G4; additional microbiology data for known G4 binders BRACO-19, TMPyP4, and RHPS4; physicochemical and ADME descriptors for compounds 1–13 and for reference G4 binders used in this work; experimental details on molecular modeling, CD studies, and microbiology investigations (PDF)

■ AUTHOR INFORMATION

Corresponding Authors

Daniela Montesarchio – Department of Chemical Sciences, University of Naples Federico II, Napoli 80126, Italy; Phone: +39 081674126; Email: daniela.montesarchio@unina.it

Mattia Mori – Department of Biotechnology, Chemistry and Pharmacy, University of Siena, Siena 53100, Italy; orcid.org/0000-0003-2398-1254; Phone: +39 0577 232360; Email: mattia.mori@unisi.it

Authors

Martina Fiabane – Department of Biotechnology, Chemistry and Pharmacy, University of Siena, Siena 53100, Italy; orcid.org/0009-0009-2438-9018

Chiara Platella – Department of Chemical Sciences, University of Naples Federico II, Napoli 80126, Italy; orcid.org/0000-0002-6997-1767

Fabiana Diaco – Department of Molecular Medicine, Laboratory of Microbiology and Virology, Sapienza University of Rome, Rome 00185, Italy

Cristiano Biancucci – Department of Chemistry and Technology of Drugs, Sapienza University of Rome, Rome 00185, Italy

Andrea Calcaterra – Department of Chemistry and Technology of Drugs, Sapienza University of Rome, Rome 00185, Italy; orcid.org/0000-0001-7036-6620

Domenica Musumeci – Department of Chemical Sciences, University of Naples Federico II, Napoli 80126, Italy; Institute of Biostructures and Bioimaging (IBB) - CNR, Napoli 80145, Italy; orcid.org/0000-0001-7624-1933

Guido Antonelli – Department of Molecular Medicine, Laboratory of Microbiology and Virology, Sapienza University of Rome, Rome 00185, Italy

Ombretta Turriziani – Department of Molecular Medicine, Laboratory of Microbiology and Virology, Sapienza University of Rome, Rome 00185, Italy

Bruno Botta – Department of Chemistry and Technology of Drugs, Sapienza University of Rome, Rome 00185, Italy; orcid.org/0000-0001-8707-4333

Complete contact information is available at:

<https://pubs.acs.org/10.1021/acsmchemlett.5c00428>

Author Contributions

▽ M.F., C.P., and F.D. contributed equally to this study.

Funding

This study has received funding from the European Union - Next Generation EU, Mission 4 Component 1, CUP B53D2302560 0001 (PI: A.C.), CUP B53D2302561 0001 (PI: M.M.), and CUP E53D2301591 0001 (PI: D.M.), project P2022BWS27 G4MICRONAT, and partially from the EU's Next Generation EU-MUR PNRR Extended Partnership initiative on Emerging Infectious Diseases (project no. PE00000007, INF-ACT) to M.M. and M.F.

Notes

Safety considerations: No unexpected or unusually high safety hazards were encountered.

The authors declare no competing financial interest.

ACKNOWLEDGMENTS

We thank OpenEye Cadence Molecular Sciences for their free academic license.

LIST OF ABBREVIATIONS

ADME, absorption, distribution, metabolism, and excretion; AMR, antimicrobial resistance; CD, circular dichroism; FDA, Food and Drug Administration; G4, G-quadruplex; MIC, minimal inhibitory concentration; NGS, next-generation sequencing; NMR, nuclear magnetic resonance; PDS, pyridostatin; R&D, research and development; SVD, singular value decomposition; T_m , melting temperature; WHO, World Health Organization

REFERENCES

- (1) Antimicrobial Resistance Division (AMR), Impact Initiatives and Research Coordination (IRC) WHO bacterial priority pathogens list, 2024: Bacterial pathogens of public health importance to guide research, development and strategies to prevent and control antimicrobial resistance; Antimicrobial Resistance Division (AMR), Impact Initiatives and Research Coordination (IRC): 17 May 2024; p 72.
- (2) Naghavi, M.; Vollset, S. E.; Ikuta, K. S.; Swetschinski, L. R.; Gray, A. P.; et al. Global burden of bacterial antimicrobial resistance 1990–2021: a systematic analysis with forecasts to 2050. *Lancet* **2024**, *404* (10459), 1199–1226.
- (3) Kariuki, S. Global burden of antimicrobial resistance and forecasts to 2050. *Lancet* **2024**, *404* (10459), 1172–1173.
- (4) de Kraker, M. E. A.; Stewardson, A. J.; Harbarth, S. Will 10 Million People Die a Year due to Antimicrobial Resistance by 2050? *Plos Medicine* **2016**, *13* (11), e1002184.

- (5) Plackett, B. No money for new drugs. *Nature* **2020**, *586* (7830), S50–S52.
- (6) Ardal, C.; Balasegaram, M.; Laxminarayan, R.; McAdams, D.; Otterson, K.; et al. Antibiotic development - economic, regulatory and societal challenges. *Nature Reviews Microbiology* **2020**, *18* (5), 267–274.
- (7) Hegemann, J. D.; Birkelbach, J.; Walesch, S.; Muller, R. Current developments in antibiotic discovery: Global microbial diversity as a source for evolutionary optimized anti-bacterials. *Embo Rep* **2023**, *24* (1), No. e56184.
- (8) Hoffman, P. S. Antibacterial Discovery: 21st Century Challenges. *Antibiotics (Basel)* **2020**, *9* (5), 213.
- (9) Seguin-Devaux, C.; Mestrovic, T.; Arts, J. J.; Sen Karaman, D.; Nativi, C.; et al. Solving the antibacterial resistance in Europe: The multipronged approach of the COST Action CA21145 EURESTOP. *Drug Resist Updat* **2024**, *74*, 101069.
- (10) Krajnc, A.; Brem, J.; Hinchliffe, P.; Calvopiña, K.; Panduwawala, T. D.; et al. Bicyclic Boronate VNRX-5133 Inhibits Metallo- and Serine- β -Lactamases. *J. Med. Chem.* **2019**, *62* (18), 8544–8556.
- (11) De Falco, A.; Alfano, A. I.; Cutarella, L.; Mori, M.; Brindisi, M. Harder than Metal: Challenging Antimicrobial Resistance with Metallo- β -lactamase Inhibitors. *J. Med. Chem.* **2025**, *68*, 10556.
- (12) Ciaco, S.; Aronne, R.; Fiabane, M.; Mori, M. The Rise of Bacterial G-Quadruplexes in Current Antimicrobial Discovery. *ACS Omega* **2024**, *9* (23), 24163–24180.
- (13) Neidle, S. Quadruplex nucleic acids as targets for anticancer therapeutics. *Nat. Rev. Chem.* **2017**, *1* (5), 0041.
- (14) Roy, S.; Pramanik, P.; Bhattacharya, S. Exploring the role of G-quadruplex DNA, and their structural polymorphism, in targeting small molecules for the design of anticancer therapeutics: Progress, challenges, and future directions. *Biochimie* **2025**, *234*, 120–145.
- (15) Robinson, J.; Raguseo, F.; Nuccio, S. P.; Liano, D.; Di Antonio, M. DNA G-quadruplex structures: more than simple roadblocks to transcription? *Nucleic Acids Res.* **2021**, *49* (15), 8419–8431.
- (16) Cueny, R. R.; McMillan, S. D.; Keck, J. L. G-quadruplexes in bacteria: insights into the regulatory roles and interacting proteins of non-canonical nucleic acid structures. *Crit Rev. Biochem Mol.* **2022**, *57* (5–6), 539–561.
- (17) Ahmed, A. A.; Greenhalf, W.; Palmer, D. H.; Williams, N.; Worthington, J.; et al. The Potent G-Quadruplex-Binding Compound QN-302 Downregulates S100P Gene Expression in Cells and in an In Vivo Model of Pancreatic Cancer. *Molecules* **2023**, *28* (6), 2452.
- (18) Dallavalle, S.; Artali, R.; Princiotta, S.; Musso, L.; Borgonovo, G.; Mazzini, S. Investigation of the Interaction between Anthraquinone Metabolites and G-Quadruplex DNA Structures. *Int. J. Mol. Sci.* **2022**, *23* (24), 16018.
- (19) Wang, Y.; Patel, D. J. Solution structure of the Tetrahymena telomeric repeat d(T2G4)₄ G-tetraplex. *Structure* **1994**, *2* (12), 1141–56.
- (20) Barbier, F.; Andreumont, A.; Wolff, M.; Bouadma, L. Hospital-acquired pneumonia and ventilator-associated pneumonia: recent advances in epidemiology and management. *Curr. Opin Pulm Med.* **2013**, *19* (3), 216–28.
- (21) Malhotra, S.; Hayes, D.; Wozniak, D. J. Cystic Fibrosis and *Pseudomonas aeruginosa*: the Host-Microbe Interface. *Clin Microbiol Rev.* **2019**, *32* (3), cmr.00138-18.
- (22) Breidenstein, E. B. M.; de la Fuente-Núñez, C.; Hancock, R. E. W. *Pseudomonas aeruginosa*: all roads lead to resistance. *Trends in Microbiology* **2011**, *19* (8), 419–426.
- (23) Pang, Z.; Raudonis, R.; Glick, B. R.; Lin, T. J.; Cheng, Z. Y. Antibiotic resistance in *Pseudomonas aeruginosa*: mechanisms and alternative therapeutic strategies. *Biotechnol Adv.* **2019**, *37* (1), 177–192.
- (24) Lister, P. D.; Wolter, D. J.; Hanson, N. D. Antibacterial-resistant *Pseudomonas aeruginosa*: clinical impact and complex regulation of chromosomally encoded resistance mechanisms. *Clin Microbiol Rev.* **2009**, *22* (4), 582–610.

- (25) Cigana, C.; Lore, N. I.; Riva, C.; De Fino, I.; Spagnuolo, L.; et al. Tracking the immunopathological response to *Pseudomonas aeruginosa* during respiratory infections. *Sci. Rep.* **2016**, *6*, 21465.
- (26) Jesudason, T. WHO publishes updated list of bacterial priority pathogens. *Lancet Microbe* **2024**, *5* (9), 100940.
- (27) Picarazzi, F.; Zuanon, M.; Pasqualetto, G.; Cammarone, S.; Romeo, I.; et al. Identification of Small Molecular Chaperones Binding P23H Mutant Opsin through an In Silico Structure-Based Approach. *J. Chem. Inf. Model* **2022**, *62* (22), 5794–5805.
- (28) Platella, C.; Ghirga, F.; Zizza, P.; Pompili, L.; Marzano, S.; et al. Identification of Effective Anticancer G-Quadruplex-Targeting Chemotypes through the Exploration of a High Diversity Library of Natural Compounds. *Pharmaceutics* **2021**, *13* (10), 1611.
- (29) Ciaco, S.; Mazzoleni, V.; Javed, A.; Eiler, S.; Ruff, M.; et al. Inhibitors of UHRF1 base flipping activity showing cytotoxicity against cancer cells. *Bioorganic Chemistry* **2023**, *137*, 106616.
- (30) Verdonk, M. L.; Cole, J. C.; Hartshorn, M. J.; Murray, C. W.; Taylor, R. D. Improved protein-ligand docking using GOLD. *Proteins* **2003**, *52* (4), 609–23.
- (31) Platella, C.; Mazzini, S.; Napolitano, E.; Mattio, L. M.; Beretta, G. L.; et al. Plant-Derived Stilbenoids as DNA-Binding Agents: From Monomers to Dimers. *Chem. Eur. J.* **2021**, *27* (34), 8832–8845.
- (32) Scott, L.; Chalikian, T. Stabilization of G-Quadruplex-Duplex Hybrid Structures Induced by Minor Groove-Binding Drugs. *Life-Basel* **2022**, *12* (4), 597.
- (33) Collie, G. W.; Parkinson, G. N. The application of DNA and RNA G-quadruplexes to therapeutic medicines. *Chem. Soc. Rev.* **2011**, *40* (12), 5867–5892.
- (34) Savva, L.; Georgiades, S. N. Recent Developments in Small-Molecule Ligands of Medicinal Relevance for Harnessing the Anticancer Potential of G-Quadruplexes. *Molecules* **2021**, *26* (4), 841.
- (35) Platella, C.; Ghirga, F.; Musumeci, D.; Quaglio, D.; Zizza, P.; et al. Selective Targeting of Cancer-Related G-Quadruplex Structures by the Natural Compound Dicentrine. *Int. J. Mol. Sci.* **2023**, *24* (4), 4070.
- (36) Amato, J.; Platella, C.; Iachettini, S.; Zizza, P.; Musumeci, D.; et al. Tailoring a lead-like compound targeting multiple G-quadruplex structures. *Eur. J. Med. Chem.* **2019**, *163*, 295–306.
- (37) Tran, P. L. T.; Mergny, J. L.; Alberti, P. Stability of telomeric G-quadruplexes. *Nucleic Acids Res.* **2011**, *39* (8), 3282–3294.
- (38) Beseiso, D.; Chen, E. V.; McCarthy, S. E.; Martin, K. N.; Gallagher, E. P.; et al. The first crystal structures of hybrid and parallel four-tetrad intramolecular G-quadruplexes. *Nucleic Acids Res.* **2022**, *50* (5), 2959–2972.
- (39) Martin, K. N.; Lam, G.; Reznichenko, O.; Brunner, K. E.; Zdilla, M. J.; et al. Conformational Change in a Four-Tetrad DNA G-Quadruplex upon Intercalation of a Small-Molecule Ligand PyDH2. *Angew. Chem. Int. Edit* **2025**, e202501443.
- (40) del Villar-Guerra, R.; Trent, J. O.; Chaires, J. B. G-Quadruplex Secondary Structure Obtained from Circular Dichroism Spectroscopy. *Angew. Chem. Int. Edit* **2018**, *57* (24), 7171–7175.
- (41) Criscuolo, A.; Napolitano, E.; Riccardi, C.; Musumeci, D.; Platella, C.; Montesarchio, D. Insights into the Small Molecule Targeting of Biologically Relevant G-Quadruplexes: An Overview of NMR and Crystal Structures. *Pharmaceutics* **2022**, *14* (11), 2361.